Study of the domain structure and mechanical properties of the ethylene oxide endcapped poly(propylene oxide) polyol/4,4′-diphenylmethane diisocyanate/ethylenediol polyurethane system

Gengchao Wang*, Bin Fang and Zhiping Zhang
Institute of Material Science and Engineering, East China University of Chemical Technology, Shanghai 200237, People's Republic of China
(Received 29 September 1992; revised 4 January 1994)

Polyurethanes from a system consisting of ethylene oxide endcapped poly(propylene oxide) polyol (PPO-EO), 4,4′-diphenylmethane diisocyanate (MDI) and ethylenediol (EDO) have been synthesized using a one-step process. The morphology of these polyurethanes has been investigated by a variety of techniques. Hard-segment-rich spherulites, with sizes of 10 μm in diameter, consisting of scattering fibrils, have been observed. The melting points of these spherulites lie in the range 220–260°C. The degree of microphase separation and the crystallinity of the polyurethanes increases with an increase in the hard-segment content. In addition, a relationship between the microstructure and the mechanical properties of these materials has been found.

(Keywords: polyurethanes; electron microscopy; domain structure)

INTRODUCTION

Various favourable properties of polyurethanes can be obtained by microphase separation and the presence of domains[1–5]. Hard-segment domains strengthen the materials by physical crosslinking, which is brought about by the presence of hydrogen bonding and crystalline regions. Therefore, the study of microphase separation and domain structure in polyurethanes is very important. Much work on the microstructure in polyether/4,4′-diphenylmethane diisocyanate (MDI)/butanediol (BDO) polyurethanes has been carried out by using differential scanning calorimetry (d.s.c.), transmission electron microscopy (TEM) and other techniques[6–8]. Two scales of structural organization were observed: (1) of the order of tens of μm, corresponding to hard-segment-rich 'globules' (HSG) and hard-segment-rich spherulites (HSS); and (2) of the order of 100 Å, associated with hard-segment-rich fibrils (HSF). The size and number of these microstructures depends on the hard-segment content, the degree of mixing and the temperature history. Although polyurethanes, chain extended with EDO, have been produced in reaction injection moulding (RIM) processes, very few studies of the microstructure of these polyurethanes have been carried out.

In an effort to better understand these EDO chain extended materials, a series of polyurethane samples, derived from the ethylene oxide endcapped poly(propylene oxide) polyol/4,4′-diphenylmethane diisocyanate/ethylenediol (PPO-EO/MDI/EDO) system, were prepared by a hand casting procedure. The crystals and domain structures in these polyurethanes have been characterized, and the influence of the microstructures on the mechanical properties of the materials discussed.

EXPERIMENTAL

Materials

Poly(propylene oxide) polyol, endcapped with ethylene oxide (PPO-EO) (Dow Chemical Corporation), with a functionality of 3.05 and $M_n = 3100$, was dried under vacuum in the presence of molecular sieves. 4,4′-Diphenylmethane diisocyanate (MDI), supplied by the Yantai Leatherette Factory, was filtered at 60°C. Ethylenediol (EDO), produced by the Shanghai Chemical Agent Factory, was vacuum distilled and then dried over molecular sieves.

Stoichiometric amounts of PPO-EO and EDO were charged into a 250 ml reaction vessel and stirred for 10 min at 60°C under nitrogen. A 5% molar excess (over the stoichiometric amount) of molten MDI (at 60°C) was then added. The mixture was stirred for 10 min at 2000 rev min^{-1} and then degassed under vacuum for 5 min. The reaction mixture was poured into a preheated glass mould and the latter was heated in an oven at 100°C for 20 h. Five different polyurethane samples with hard segment concentrations ranging from 11 to 47 wt% were produced in this way (*Table 1*).

Differential scanning calorimetry (d.s.c.)

A Du Pont 1090 thermal analyser was used to examine the thermal properties of the samples. D.s.c. scans of all

* To whom correspondence should be addressed

0032-3861/94/15/3178–06

Table 1 Chemical composition and hard-segment content of samples of the PPO-EO/MDI/EDO series of polyurethanes

Sample	PPO-EO/MDI/EDO (mole ratio)	Hard-segment content (wt% (h))
M-E-0	1/1.05/0	11
M-E-1	1/2.10/1	24
M-E-2	1/3.15/2	34
M-E-3	1/4.20/3	41
M-E-4	1/5.25/4	47

of the samples were obtained over a temperature range of -100 to 280°C, using a heating rate of 10°C min^{-1}. The sample weight was $\sim$10 mg.

Wide-angle X-ray diffraction (WAXD)

WAXD studies were carried out using a Rigaku D/MAX-RB X-ray diffractometer, employing nickel-filtered CuKα radiation. The 2θ scan rate was 4° min^{-1}. Diffractometer scans were run in the reflection mode on plaques (3.00 mm thick) of the as-polymerized samples.

Electron microscopy

Scanning electron microscopy (SEM) studies were carried out on a JEM-200CX instrument operating at 20 kV. Samples were etched for a week with DMF vapour, and were then sputter coated with a layer of gold ($\sim$300 Å thick).

Transmission electron microscopy (TEM) investigations were carried out using a JEM-200CX machine operating at 100 kV. The specimens were enclosed in epoxy resin and cut into ultrathin sections. These microtomed specimens, after staining with RuO_4, were examined on copper grids (300 mesh) without any supporting film.

Mechanical properties

Tensile strength and ultimate elongation were measured using a Shengdei DL-250 screw-driven testing machine, at an elongation rate of 200 mm min^{-1}. Hardness tests were performed by using a Shanghai Luzhong LX-A rubber hardness tester.

RESULTS AND DISCUSSION

Differential scanning calorimetry

Figure 1 shows the d.s.c. curves obtained for PPO-EO and the various polyurethanes with different hard-segment contents. It can be seen that the polyurethane samples exhibit two glass transition temperatures (T_gs) and several endothermic peaks. The lower T_g (T_g(s)) was associated with the soft-segment phase and the other T_g (T_g(h)) was associated with the hard-segment domain[9]. It was found from the T_g data (see *Table 2*) that they tend to shift outwards as the content of hard segments increased. This suggested that with an increasing hard-segment content the miscibility of the hard and soft segments decreases, and therefore the degree of microphase separation increases. It can also be seen that with an increasing hard-segment content the number of endothermic peaks for the polyurethanes increases. For all of the samples, two small and sharp endothermic peaks (at -15 and 41°C) were observed in the d.s.c. scans. These were almost certainly associated with the soft segments, because the same two peaks can also be observed for the PPO-EO sample (see curve (a)) which contains no hard

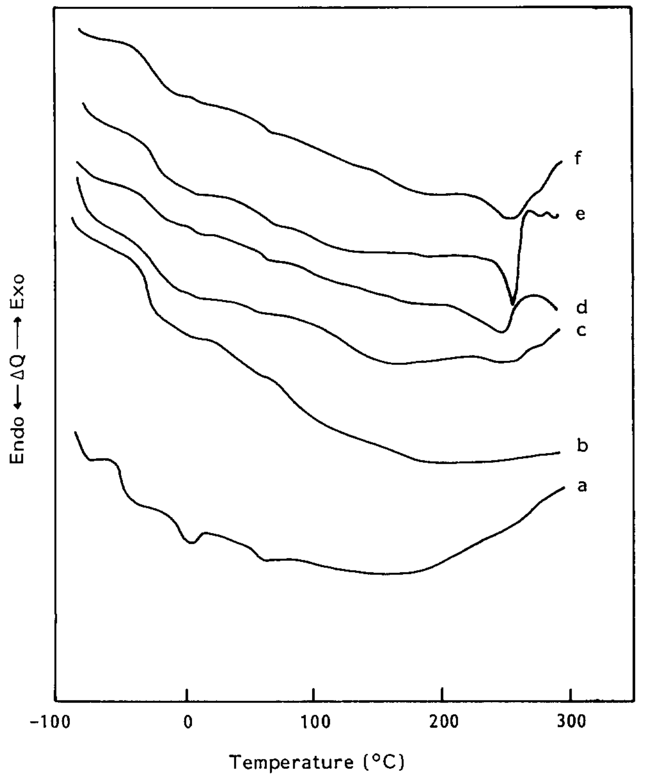

Figure 1 D.s.c. curves of the PPO-EO/MDI/EDO series of polyurethanes: (a) PPO-EO; (b) M-E-0; (c) M-E-1; (d) M-E-2; (e) M-E-3; (f) M-E-4

Table 2 Thermal data obtained from d.s.c. measurements on PPO-EO and samples of the PPO-EO/MDI/EDO series of polyurethanes[a]

Sample	T_g (s)	T_m (s)	T_g(h)	T_1	T_m (h)
PPO-EO	-66	-15, 41	–	–	–
M-E-0	-40	-15, 41	64	–	–
M-E-1	-41	-15, 41	84	–	223
M-E-2	-41	-15, 41	82	166	227
M-E-3	-42	-15, 41	85	165	228, 240, 260
M-E-4	-43	-15, 41	87	163	225, 242, 260

[a] All temperatures in °C

segments. For a sample with a low content of hard segments (11 wt%) the d.s.c. plot shows no high-temperature endothermic peaks (curve (b)). For the sample with an 'intermediate' level of hard-segment content (24 wt%), the melting peaks of the hard-segment crystals can be observed over the range 200–260°C (curve (c))[10]. In addition to the peaks described above, those samples with hard-segment contents greater than 34 wt% exhibit a new endothermic peak at $\sim$165°C (see curves (d), (e) and (f)). This new peak was previously observed by Srichatrapimuk and Cooper and was described as being due to disordering of the ordered structure in the hard-segment domains[9].

Wide-angle X-ray diffraction

Figure 2 shows the wide-angle X-ray diffraction patterns that were obtained for this series of polymers. All of the polyurethanes exhibit many diffraction peaks; the Bragg spacings are listed in *Table 3*. Sample M-E-0,

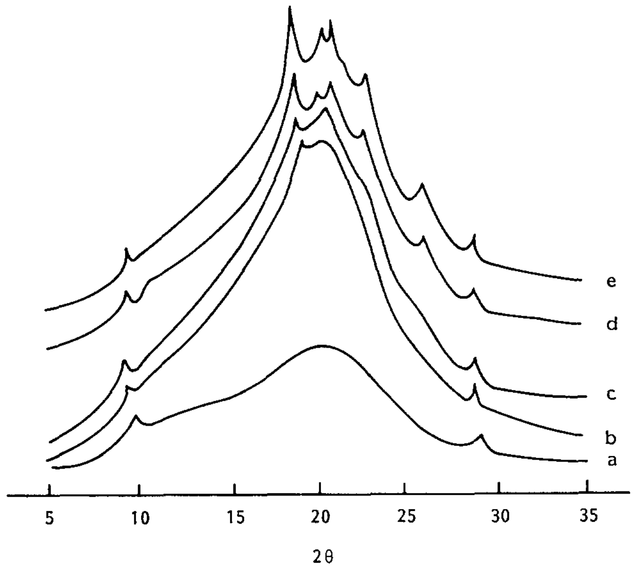

Figure 2 WAXD scans of the PPO-EO/MDI/EDO series of polyurethanes: (a) M-E-0; (b) M-E-1; (c) M-E-2; (d) M-E-3; (e) M-E-4

Table 3 Bragg spacings of the WAXD peaks for the PPO-EO/MDI/EDO series of polyurethanes[a]

No.	M-E-0	M-E-1	M-E-2	M-E-3	M-E-4
1[b]	9.33	9.33	9.33	9.33	9.33
2	–	4.90	4.90	4.90	4.90
3	–	–	–	–	4.33
4	–	–	4.26	4.26	4.26
5	–	–	–	3.97	3.97
6	–	–	–	3.51	3.51
7[b]	3.22	3.22	3.22	3.22	3.22

[a] Distances in Å
[b] 9.33 and 3.22 Å are the Bragg spacings associated with the soft-segment crystals

in which no hard-segment crystals were observed by d.s.c. measurements (see curve (b) in *Figure 1*) shows only two small and sharp diffraction peaks (see curve (a)) at 9.33 and 3.22 Å. Therefore, the two peaks found in *Figure 2* for all of the samples were attributed to the soft-segment crystals, with the other peaks being associated with the hard-segment crystals. *Figure 2* also shows that the number and intensity of the diffraction peaks of the hard-segment crystals increases with increasing hard-segment content. This indicated that the crystallinity increases with the increase in hard-segment content, a result which is quite consistent with the d.s.c. observations.

To form hard-segment crystals in the MDI polyurethane system the segments need to be of a sufficient length. It is known that hard segments consisting of more than three MDI units can produce stable crystals[11]. For the sample M-E-0, no hard-segment-crystal diffraction peak was observed in the WAXD plot, which is consistent with the d.s.c. results. This is because every hard segment in the M-E-0 sample, which contains no EDO chain extender, consists of only one MDI unit. For the sample M-E-1, however, the small peak at 4.90 Å in the WAXD curve indicated the presence of hard-segment crystals although the hard segment contains, on average, two MDI units. This can be understood as follows. In polyurethanes produced by a one-step process, the hard-segment length distribution is very wide, so part of the hard segments contains more than the three MDI units needed to produce crystals. For the polyurethanes with an increased content of hard segments, such as M-E-2, M-E-3 and M-E-4, the average hard-segment length increases and thus the crystallinity is considerably enhanced.

Scanning electron microscopy

Figure 3 shows scanning electron micrographs of these polyurethanes after etching with DMF vapour. The extent of etching in the soft- and hard-segment domains differs. The soft-segment domains can be etched more easily, so it is reasonable to think that the dark regions in the micrographs represent the soft-segment domains, with the bright regions representing the hard-segment domains. The morphological changes which occur with increasing hard-segment content can be clearly seen in *Figure 3*. For sample M-E-0, hard-segment-rich 'globules' which disperse in the soft-segment-rich matrix can be observed (see *Figure 3a*). As this sample contains no EDO chain extender, the hard segment is very short and the fraction of hydrogen bonding among the hard segments is low. Therefore, it is difficult to bring these segments together and form crystals. For the sample M-E-1, the hard segments form stick-like structures (see *Figure 3b*). This is because the hard segments become longer in this sample as a result of the introduction of the chain extender. For the samples with a very high content of hard segments, the latter form spherulites, whose quality is improved as the hard-segment content is increased (see *Figures 3c–3e*). This was attributed to the long sequences of hard segments in these samples, which induced strong hydrogen bond interactions among hard segments, thus forming better spherulites.

Transmission electron microscopy

In order to study hard-segment-rich crystals, polyurethanes with high hard-segment contents were examined by using TEM. *Figures 4* and *5* show, respectively, transmission electron micrographs of ultrathin sections of samples M-E-3 and M-E-4 after staining with RuO_4. The contrast between the crystalline and amorphous regions is enhanced by using the staining technique. It is reasonable to think that the bright regions in the micrographs represent the crystals, with the dark regions representing the amorphous regions. Hard-segment-rich spherulites were observed in both samples M-E-3 and M-E-4. The spherulites consist of scattering fibrils (see *Figures 4a* and *5a*). (Note that *Figures 4b* and *5b* are the same micrographs as in *Figures 4a* and *5a*, respectively, but at a higher magnification.) The thickness of the fibrils varies from 6 to 14 nm. As the spherulitic structure of these polyurethanes has not yet been perfected, irregular lamellae can exist within the boundaries of the spherulites: the thickness of these lamellae is ~10 nm (see *Figure 5c*). *Figure 5d* shows the interface between a spherulite and the amorphous region.

Mechanical properties

Figure 6 shows the tensile strength, ultimate elongation and hardness as a function of the hard-segment content in these polyurethanes, with the experimental data given in *Table 4*. *Figure 6* indicates that both the tensile strength and the hardness increase with increasing hard-segment

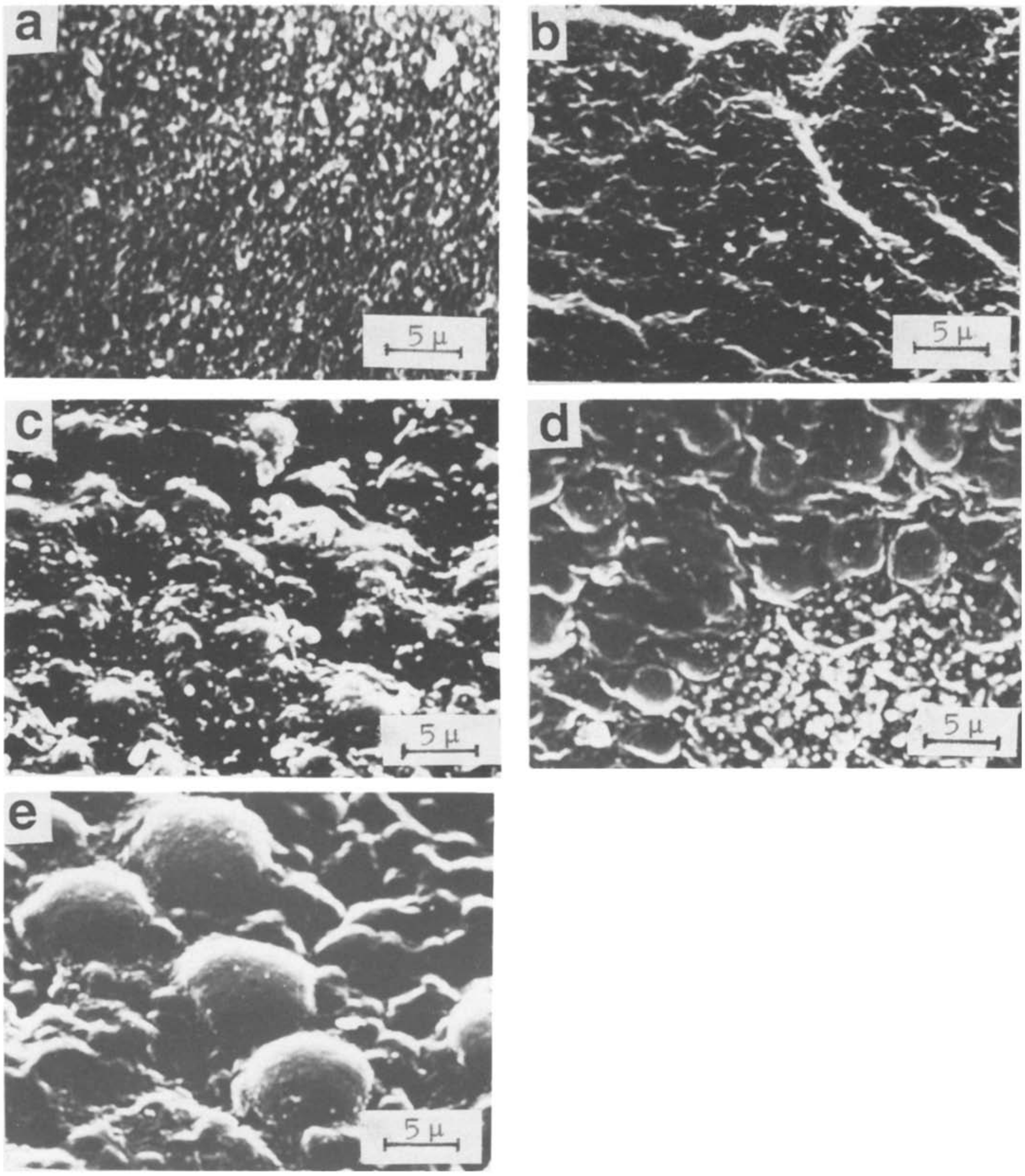

Figure 3 Scanning electron micrographs of the PPO-EO/MDI/EDO series of polyurethanes after etching with DMF vapour: (a) M-E-0, 11 wt% hard segment; (b) M-E-1, 24 wt% hard segment; (c) M-E-2, 34 wt% hard segment; (d) M-E-3, 41 wt% hard segment; (e) M-E-4, 47 wt% hard segment

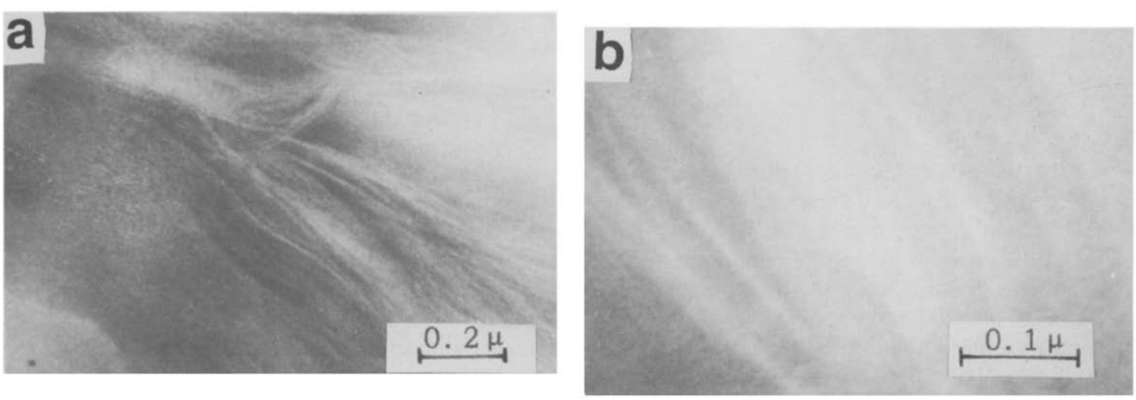

Figure 4 Transmission electron micrographs of an ultrathin section of polyurethane sample M-E-3, after staining with RuO_4, showing (a) spherulites and (b) fibrils

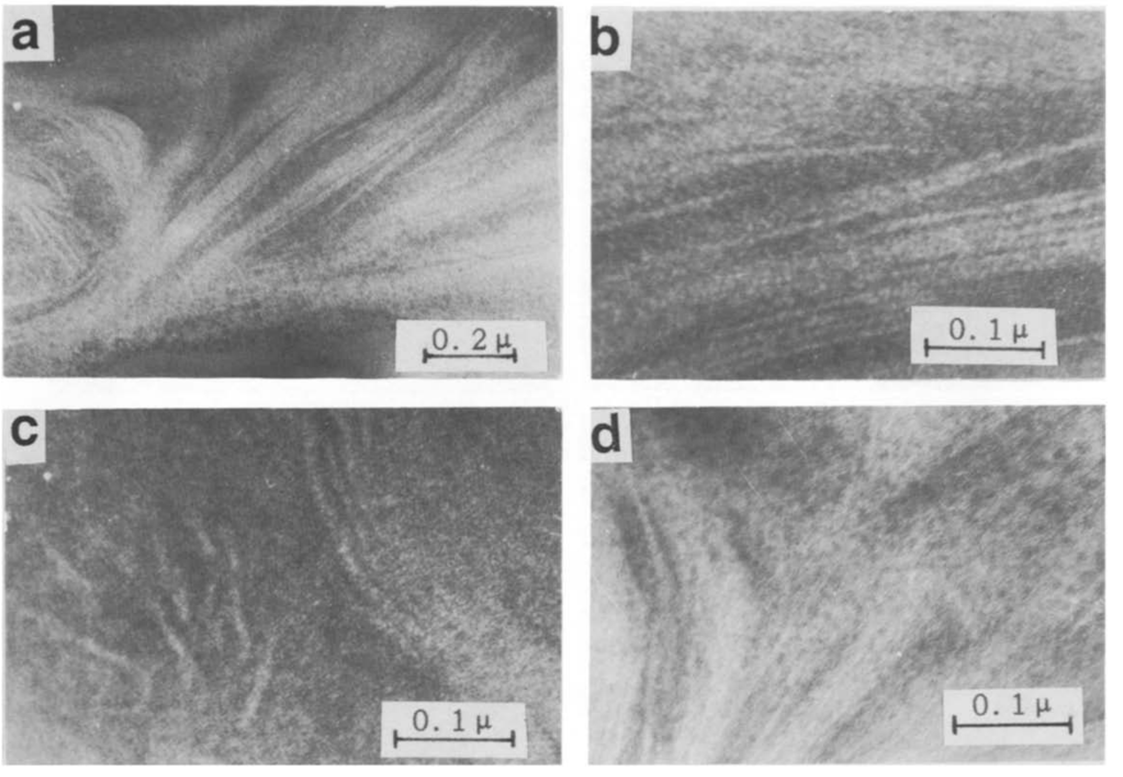

Figure 5 Transmission electron micrographs of ultrathin sections of polyurethane sample M-E-4, after staining with RuO_4, showing: (a) spherulites; (b) fibrils; (c) lamellae contained within the boundaries of the spherulites; (d) interface between a spherulite and the amorphous region

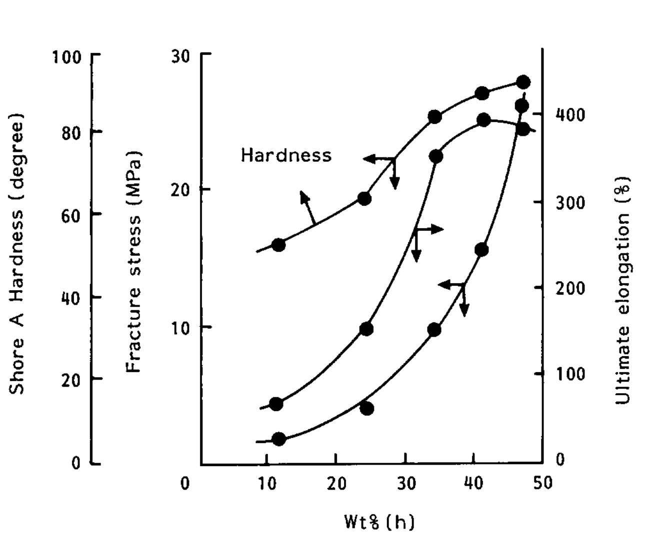

Figure 6 Tensile stress, ultimate elongation and hardness as a function of hard-segment content for PPO-EO/MDI/EDO series of polyurethanes

content, as a result of the degree of microphase separation of the hard and soft segments and the crystallinity in the hard-segment domains being enhanced. A rapid increase in hardness is found in the hard-segment content range from 25 to 35 wt%, because of a sudden increase in crystallinity. It can also be seen in *Figure 6* that the ultimate elongation goes through a maximum at a hard-segment content of ~40%. The above types of behaviour are caused by two opposing effects. First, the soft segments can aggregate easily with increases in the hard-segment content, so that the toughness and ultimate elongation are enhanced. Secondly, an increase in crosslinking density, which impedes movement of the soft segments, with increases in the hard-segment content, has the effect of decreasing the ultimate elongation.

Table 4 Mechanical properties data for samples of the PPO-EO/MDI/EDO series of polyurethanes

Sample	Tensile stress (MPa)	Ultimate elongation (%)	Shore A hardness (degree)
M-E-0	1.5	72.2	54
M-E-1	3.7	193.4	64
M-E-2	9.3	349.3	83
M-E-3	15.2	394.4	88
M-E-4	25.5	388.9	91

CONCLUSIONS

The domain structure and mechanical properties of PPO-EO/MDI/EDO based polyurethanes have been studied. For all of the polyurethanes studied, small amounts of crystals exist in the soft-segment domains. Hard-segment-rich spherulites, 10 μm in diameter, consisting of scattering fibrils, have been observed. The melting points of these spherulites are in the range 220–260°C. With an increasing hard-segment content the microphase separation degree and the crystallinity both increase, resulting in an enhancement of the tensile stress and the hardness. The ultimate elongation reaches a maximum at a hard-segment content of ~40 wt%. The relationship between the microstructure and the mechanical properties has been explained.

ACKNOWLEDGEMENT

We are grateful to Senior Engineer Gao Yong-qi of the Research Institute of the Liming Chemical Industry for his help with the electron microscopy work.

REFERENCES

1 Cooper, S. L. and Tobolsky, A. V. *J. Appl. Polym. Sci.* 1966, **10**, 1837
2 Bonart, R. *J. Macromol. Sci. Phys.* 1968, **2**, 115
3 Huh, D. S. and Cooper, S. L. *Polym. Eng. Sci.* 1977, **11**, 369
4 Wilkes, C. E. and Yusek, C. S. *J. Macromol. Sci. Phys.* 1973, **7**, 157
5 Chang, A. L., Briber, R. M., Thomas, E. L., Zdrahala, R. J. and Critchfield, F. E. *Polymer* 1982, **23**, 1060
6 Xu, M., MacKnight, W. J., Chen-Tsai, C. H. Y. and Thomas, E. L. *Polymer* 1987, **28**, 2183
7 Fridman, I. D. and Thomas, E. L. *Polymer* 1980, **21**, 388
8 Foks, J., Michler, G. and Nanman, I. *Polymer* 1987, **28**, 2195
9 Srichatrapimuk, V. W. and Cooper, S. L. *J. Macromol. Sci. Phys.* 1978, **B15**(2), 267
10 Blackwell, J. and Lee, C. D. *J. Polym. Sci. Polym. Phys. Edn* 1984, **22**, 759
11 Chan, K. W. and Geil, P. H. *Polymer* 1985, **26**, 490